Electrochimica Acta 508 (2024) 145259

Contents lists available at ScienceDirect

Electrochimica Acta

journal homepage: www.journals.elsevier.com/electrochimica-acta

Water electrolysis using fluorine-free, reinforced sulfo-phenylated polyphenylene membranes

Franklin O. Egemole [a], Ana Laura G. Biancolli [a,b], Steven Holdcroft [a,*]

[a] Department of Chemistry, Simon Fraser University, Burnaby, BC, V5A 1S6, Canada
[b] Nuclear and Energy Research Institute, IPEN/CNEN, 05508-000, São Paulo, Brazil

ARTICLE INFO

Keywords:
Proton-exchange membrane water electrolysis
Green hydrogen
Catalyst coated membranes
Reinforced membrane
Pemion™
Sulfo-phenylated polyphenylene

ABSTRACT

Fluorinated proton-exchange membranes (PEMs), such as Nafion™, which is the current state-of-the-art polymer, present environmental challenges, driving the need for more sustainable alternatives for proton-exchange membrane water electrolysis (PEMWE) systems. However, fluorine-free membranes like sulfo-phenylated polyphenylene biphenyl (sPPB-50) often suffer from mechanical instability, excessive swelling, and limited cell durability, which hinder their practical applications. This study explores reinforced fluorine-free sulfo-phenylated polyphenylene membranes (Pemion™) with thicknesses of 15 μm (Pemion-15) and 40 μm (Pemion-40) as a potential solution to these issues. Pemion membranes were compared with both sPPB-50 and Nafion™ 112 (N112), focusing on key properties such as water uptake, dimensional swelling, proton conductivity, and durability in PEMWE applications. The results show that Pemion-reinforced membranes exhibit good performance for PEMWE allowing high current densities at lower voltages. Pemion-40 exhibited a low hydrogen gas crossover compared to sPPB-50 and N112. Under a constant current of 1 A cm^{-2}, Pemion-40 exhibited a voltage loss rate of 1.46 mV h^{-1} over 100 h of operation. This study highlights the importance of structural reinforcement in enhancing the stability and efficiency of fluorine-free membranes, providing a promising route for sustainable alternatives in PEMWE systems.

1. Introduction

In addition to fuel cell technology, proton-exchange membranes (PEM) have gained increasing attention due to their potential use as solid polymer electrolytes in proton-exchange membrane water electrolysis (PEMWE) for producing high-purity hydrogen [1–5]. The use of thin membranes in PEMWE reduces ohmic losses at high current densities, thereby leading to high energy efficiencies [6–8]. Perfluorosulphonic acid (PFSA) based membranes, such as Nafion™, are the technological and commercial standard, as they offer the combination of stability, proton conductivity, mechanical strength, and they are widely available [9–11]. Their drawbacks include toxicological concerns surrounding their manufacture, and high hydrogen crossover because of the combined high gas solubility and diffusivity [12–14]. As in the corollary case of PEM fuel cells, robust, fluorine-free, membranes are highly sought after since fluorine-free polymers often possess an inherent lower gas permeability, higher proton conductivity, higher glass transition temperature, and can be produced from environmental-friendly feedstocks [15–17].

Several reports focusing on investigating fluorine-free polymers (often referred to as *hydrocarbon* PEMs) as solid polymer electrolyte membranes for PEMWE applications have been reported [18–21]. The significant drawback, however, is that all fluorine-free PEMs to date exhibit much lower stability during water electrolysis than incumbent PFSA ionomer membranes due to their inherent poor mechanical properties, which are exacerbated by their intrinsic chemical instabilities and excessive swelling [22–24]. Several strategies have been employed to increase the mechanical stability of fluorine-free PEMs. These include chemical strategies such as chemical crosslinking, or physical reinforcement such as the introduction of nanoparticles or reinforcing layers to produce nanocomposite membranes [25–27]. For example, the incorporation of mechanically robust porous poly(tetrafluoroethylene) (PTFE) into sulfonated poly(arylene ether sulfone) (SPAES) ionomer was reported to have resulted in improved dimensional and mechanical properties compared to the pristine membrane, while also lowering the voltage degradation rate during a 100-hour durability test at a constant current of 2 A cm^{-2} [27]. Another work reported a composite hydrocarbon membrane made from sulfonated

* Corresponding author.
E-mail address: holdcrof@sfu.ca (S. Holdcroft).

https://doi.org/10.1016/j.electacta.2024.145259
Received 9 April 2024; Received in revised form 16 September 2024; Accepted 18 October 2024
Available online 20 October 2024

poly(arylene ether sulfone) with a sulfonation degree of 50 mol% (SPAES50) reinforced with liquid crystal polymer (LCP)-nonwoven fabrics that demonstrated superior mechanical strength, dimensional stability, and enhanced cell efficiency and durability compared to the pristine hydrocarbon membrane in PEMWE [28].

We have reported extensively on the use of fluorine-free, proton-conducting sulfo-phenylated polyphenylene biphenyl membranes (sPPB-H^+, Fig S1) in fuel cells [29,30], demonstrating beginning of life performance comparable to PFSA ionomer membranes. The performance and durability of those membranes are rapidly improving [31], to the point they are being considered as replacements for PFSA ionomers in some applications [32]. It is logical, therefore, to examine similar materials in PEMWE applications. In this context, sPPB-H^+ membrane (50 μm of dry thickness, sPPB-50) was used in a PEM water electrolyzer and reported to support a current density of 1 A cm^{-2} at 1.66 V [33]. The sPPB-50 PEM exhibited a high proton conductivity which resulted in a lower ohmic resistance when compared to Nafion-112™ (N112) membrane of similar thickness (50 μm). However, like other non-PFSA based PEM electrolyzers, the cell durability was lower than the N112-based electrolyzer. At an operational current density of 1 A cm^{-2}, the voltage rose by 2–3 mV h^{-1} over the first 40 h, while hydrogen crossover reached >2.5 vol% within 60 h [33]. This was attributed to the lower mechanical strength and excessive swelling of the sPPB-50 membrane, which also resulted in the delamination of the catalyst layers. Since this initial work, sulfo-phenylated polyphenylene-based PEMs have been commercialized under the trade name *"Pemion"* by Ionomr Innovations Inc.. Reinforced versions, "Pemion™ reinforced", are also available and have been reported to have enhanced *ex-situ* thermo-mechanical stability, exhibiting a temperature-independent Young's modulus and strain hardening, maintaining stability at 110–120 °C and 40–50 % RH [34].

The objective of the current study is to address these durability issues by investigating reinforced versions of fluorine-free membranes, particularly "Pemion-reinforced membranes". The reinforcement layer is intended to enhance mechanical stability and mitigate the durability issues identified in the previous study, ultimately establishing fluorine-free membranes as a feasible alternative for PEMWE applications. The advancement of fluorine-free Pemion-reinforced membranes by enhancing their mechanical stability and operational efficiency for water electrolysis supports the UN Sustainable Development Goals - SDG 7 (Affordable and Clean Energy) and SDG 13 (Climate Action) - by providing a sustainable substitute for traditional fluorinated PEMs, which are viewed as potentially environmentally harmful [35].

Two thicknesses of Pemion-reinforced provided by Ionomr Innovations Inc. were studied, 15 and 40 μm (Pemion-15 and Pemion-40, respectively), and compared to non-reinforced sPPB-50 membrane, previously synthesized in-house, and N112, in the context of water uptake, dimensional swelling, and proton conductivity. Subsequently, the water electrolyzer performance, hydrogen gas crossover, and durability of corresponding catalyst-coated membranes (CCMs) in 5 cm^2 single cells were evaluated. The present work investigates Pemion-reinforced membranes as part of the effort to introduce fluorine-free membranes in electrochemical devices, which is a significant progression towards more sustainable and cost-efficient hydrogen production technologies. This research enhances the performance and durability of these membranes with the introduction of a reinforcement layer, contributing to the advancement of ongoing research on fluorine-free PEMs for water electrolysis, emphasizing the critical role of structural reinforcement in optimizing stability within such electrochemical systems.

2. Experimental details

The experimental **ion-exchange capacity (IEC)** values of the Pemion-15 and Pemion-40 membranes were determined by the acid-base titration method using an auto titrator (Metrohm 848 Titrino Plus) and calculated using Eq. S1, as described elsewhere [36].

The **water uptake (WU) and dimensional swelling** of the membranes were determined by calculating the weight (W) and dimensional changes in area (A) and thickness (T) between their dry and wet states at room temperature (RT) using Eq. S2, Eq. S3, and Eq. S4.

The **through-plane proton conductivities** of the fully hydrated membranes were obtained using an in-house built two-point probe through-plane cell controlled with a dual-rod guided air cylinder at a constant gas pressure of 60 psi. To measure the membrane's resistance, electrochemical impedance spectroscopy (EIS) analyses were carried out using Solartron S1 1260 Impedance/Gain-Phase Analyzer and operated via a galvanostatic method with an AC amplitude of 0.1 mA over a frequency range of 10 MHz to 100 Hz at RT. The ionic conductivity values (S cm^{-1}) were calculated by Eq. S5 using the membrane thickness, its surface area, and the measured ionic resistance. More information on the through-plane conductivity measurements is given in the supplementary information (SI).

Membrane/electrode assemblies (MEAs) containing Pemion-15, Pemion-40, and Nafion-112™ (N112) membranes were fabricated by the **catalyst-coated membrane (CCM)** method [37]. Catalyst inks for both electrodes were prepared as previously reported [33] and described in detail in the SI. All CCMs contained 3.0 ± 0.4 mg cm^{-2} of Ir in the anode and 1.0 ± 0.1 mg cm^{-2} of Pt in the cathode. **Water electrolysis analyses** were performed by sandwiching CCMs in a 5 cm^2 electrolysis cell (FuelCellStore, USA) using Ti felt as the porous transport layers (PTL) and Ice Cube Sealing, 35 FC-PO 100 (QuinTech, Germany) as the gaskets in the anode and cathode compartments. Electrochemical measurements were conducted using a Greenlight Innovation E20 water electrolysis test station equipped with a Gamry Interface 5000 potentiostat. Deionized water (< 0.5 μS cm^{-1}) was fed at a rate of 200 mL min^{-1} to the anode and cathode compartments of the cell at a temperature of 70 °C under ambient pressure. The cell conditioning, polarization curves, EIS, durability (100 h), and gas crossover tests were performed as reported [33]. A detailed description of the experimental methods is provided in the SI.

Scanning electron microscopy (SEM) cross-sectional images of the CCMs were taken before and after the durability studies using a FEI Nova NanoSEM 430 SEM system at an accelerating voltage of 5 kV and a working distance of 10 mm to observe any catalyst delamination. The SEM samples were prepared by freeze fracturing the CCMs in liquid nitrogen.

3. Results and discussion

Water uptake (WU) and dimensional swelling of proton-exchange membranes are influenced by the nature of the polymer or composite, the ion-exchange capacity (IEC), the method of the membranes' casting, and the thermal history of the membrane [27,38]. In this work, these properties were determined by the nature of the polymer received, and, as in the vast majority of membrane studies, no provision was made to take into account considerations of the casting and thermal history. The thickness, IEC, WU, and dimensional swelling of the membranes are listed in Table 1. Pemion-15 and Pemion-40 possessed IEC values of 2.56 and 2.85 mmol g^{-1}, respectively, which are at least 2.5 times higher than N112. The values were slightly lower than the previous published sulfo-phenylated polyphenylene biphenyl, sPPB-50 PEMs (IEC = 3.19 mmol g^{-1}) [36]. The greater IECs values observed in non-PFSA membranes result from the necessity of hydrocarbon polymers to have a significantly higher number of functional groups to establish a continuous ionic path within the membrane [32,39]. The increased WU and through-plane swelling (S_z) in Pemion-15 and Pemion-40, as compared to N112, is consistent with their higher IEC and the absence of highly hydrophobic perfluorinated chains [40]. On the other hand, Pemion-15 and Pemion-40 exhibited reduced WU and in-plane swelling ($S_{x,y}$) when compared to sPPB-50, with $S_{x,y}$ values similar to that of N112. This feature ensures enhanced mechanical stability on the in-plane direction, and it is attributed to the reinforcement within the membranes [41,42].

Table 1
Properties of membranes used in this study at room temperature (RT).

PEM	Dry thickness (μm)	Wet thickness (μm)	IEC (mmol g^{-1})	WU (%)	Sz (%)	Sx,y (%)
N112	50 ± 1	56 ± 2	0.92 ± 0.02	12 ± 1	14 ± 1	15 ± 1
Pemion-15	15 ± 1	29 ± 2	2.56 ± 0.06	107 ± 2	89 ± 3	11 ± 1
Pemion-40	40 ± 3	75 ± 3	2.85 ± 0.06	104 ± 11	88 ± 5	17 ± 1
sPPB-50	46 ± 1	79 ± 1	3.19 ± 0.05*	132 ± 7	72 ± 1	25 ± 1

WU: Water uptake of fully hydrated membranes at RT.
Sz: Through-plane swelling, *z*-direction, of fully hydrated membranes.
Sx,y : In-plane swelling, *x,y*-direction, of fully hydrated membranes.
* Data from reference [36].

Proton transport in a water electrolyzer occurs in the through-plane direction of the membrane, thus through-plane proton-conductivities of the PEMs under fully hydrated conditions at RT (~25 °C) were determined and are shown in Fig. 1a. The conductivity of each membrane at RT is calculated using the area-specific high frequency resistance (Eq. S5), which is displayed in Fig. 1b. The through-plane conductivity of polymer electrolytes is highly dependent on the cell design [43], and significantly variable with the pressure in the wet state [44]. In addition, anisotropic behaviour has been observed in several literature reports on the proton conductivity of PEMs, with in-plane conductivity values typically different from the through-plane conductivity values [45,46]. In this work, membranes were measured in both directions through-plane and in-plane. The in-plane proton-conductivities of the Pemion membranes under fully hydrated conditions at 30 °C and 70 °C are shown in Fig. S2 and compared to N112. The through-plane conductivities of the three hydrocarbon membranes (Fig. 1) possess similar values at RT (124–130 mS cm^{-1}) and are at least three times greater than the N112 value (37 mS cm^{-1}), which is consistent with their high IEC and WU at RT [47,48]. The through-plane conductivity of the N112 membrane obtained is within the range of literature conductivity results where different pressures were applied (16–45 mS cm^{-1}) [44]. It is worth noting that the structural reinforcement layer integrated into Pemion-15 and Pemion-40 membranes does not compromise their ionic conductivity. This is supported by the comparable values of ionic conductivity observed in Pemion-15 and Pemion-40, and the non-reinforced sPPB-50 membranes. A recent report [49] observed the same behaviour in the through-plane ionic conductivity of a multilayered PTFE-reinforced hydrocarbon membrane consisting of a sulfonated (arylene ether sulfone) (SPAES) copolymer with 50 % degree of sulfonation (SPAES50). The ionic conductivity of pristine SPAES50 was reported to be 158 mS cm^{-1} at 80 °C and 100 % RH, while the multilayered PTFE-reinforced SPAES50 possessed a similar value of 149 mS cm^{-1}. To minimize the decrease in ionic conductivity, the hydrocarbon ionomer should be able to effectively penetrate through the reinforcement layer, even if it is made of a non-conductive material [49].

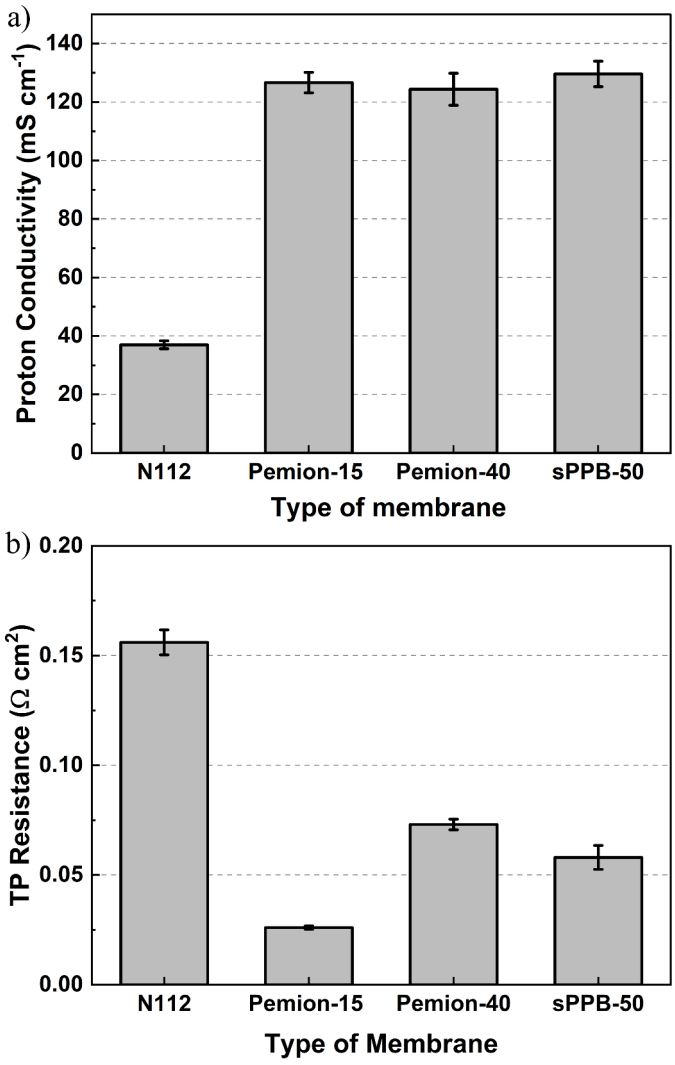

Fig. 1. a) Through-plane proton conductivity of Pemion-15, Pemion-40, sPPB-50, and N112 membranes measured ex-situ under fully hydrated conditions at RT. b) The ex-situ determined through-plane resistance of the various membranes at RT.

Pemion-15 and Pemion-40 PEMs were examined in a single water electrolysis cell (5 cm^2) and their performances were compared to N112 in Fig. 2a. The standard deviation between three measurements of identical samples is represented by the error bars in the plot. sPPB-50 membrane was examined in a previous work [33], and the reported data was added to the Figure for reference. All the CCMs were fabricated using Nafion™ D520 dispersion in the catalyst layer (10 wt% Nafion™ for the anode and 20 wt% for the cathode) as discussed in detail in the SI [33,50]. The resistances of the CCMs, both the ohmic resistance (R_Ω) and the charge transfer resistance (R_{CT}) were extracted from the EIS data obtained at 100 mA cm^{-2} (Fig. 2b) and are shown in Table 2.

The IV curves at 70 °C and ambient pressure (Fig. 2a) show that despite having different thicknesses, both Pemion-based MEAs (Pemion-15 and Pemion-40) exhibited similar performances for water electrolysis. In addition, Pemion-15 and Pemion-40-based MEAs allowed higher current densities at lower voltages in comparison to the N112 reference MEA (1.60 V *vs* 1.68 V at 1 A cm^{-2}, for example) under the same operating conditions. Also, the performances of cells containing Pemion-15 and Pemion-40 PEMs are improved over the sPPB-50 MEA (1.66 V *vs* 1.60 V at 1 A cm^{-2}, and 1.80 V *vs* 1.99 V at 2.9 A cm^{-2}) [33]. Two overlapping semi-circles are observed in the Nyquist plots of Fig. 2b. R_Ω was obtained from the Nyquist plot intercept on the real impedance axis in high frequency region, and R_{CT} from the difference between high-frequency intercept and low-frequency intercept on the real impedance axis [51]. Due to the catalyst layers' similar composition in both electrodes for all CCMs, R_{CT} of the catalyst layers were similar,

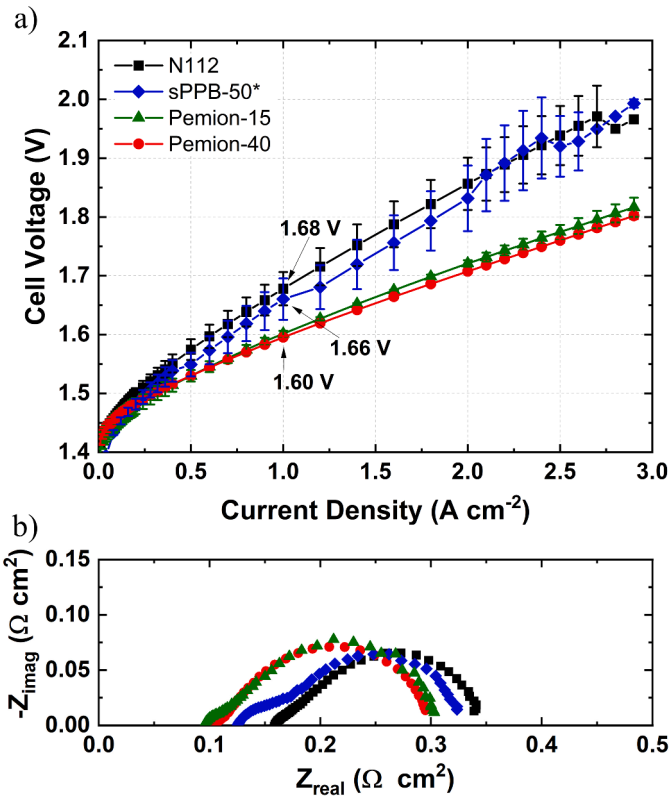

Fig. 2. Effect of membrane type in the CCMs. a) Water electrolysis polarization curves performed at 70 °C and ambient pressure with a water flow rate of 200 mL min^{-1} for Pemion-15, Pemion-40, sPPB-50, and N112 membrane CCMs. b) Nyquist plots performed at 100 mA cm^{-2} for the CCMs. All the MEAs contained ~3.0 mg Ir cm^{-2} + 10 wt% Nafion D520™ ionomer in the anode, and ~1.0 mg Pt cm^{-2} + 20 wt% Nafion D520™ ionomer in the cathode catalyst layer.
*Data from reference [33].

Table 2
Summary of the water electrolysis performance at 1 A cm^{-2} extracted from the IV curves of Fig. 2 and resistances (R_Ω and R_{CT}) obtained from the EIS analysis of CCMs based on N112, Pemion-15, Pemion-40, and sPPB-50 CCMs.

PEM	R_Ω (mΩ cm^2)	R_{CT} (mΩ cm^2)	Voltage at 1A cm^{-2}
N112	169 ± 14	189 ± 11	1.68 ± 0.03
Pemion-15	90 ± 8	199 ± 11	1.60 ± 0.01
Pemion-40	101 ± 5	180 ± 14	1.60 ± 0.01
sPPB-50*	126 ± 4	207 ± 4	1.66 ± 0.04*

* Data from reference [33].

ranging between 180 and 200 mΩ cm^2, with the main differences seen in the CCMs R_Ω values (Table 2). R_Ω of Pemion-15 CCM (90 mΩ cm^2) was 47 % lower than for N112 CCM (169 mΩ cm^2). Similarly, Pemion-40 CCM showed an ohmic resistance of 101 mΩ cm^2, which is 40 % lower compared to N112 CCM. The higher through-plane conductivity and IEC of these hydrocarbon PEMs explain the significantly lower ohmic resistance compared to N112, resulting in improved cell performance. In addition, R_Ω values of Pemion-15 and Pemion-40 CCMs were 29 % and 20 % lower, respectively, than the R_Ω of the sPPB-50 CCM (126 mΩ cm^2) [33]. Despite exhibiting similar *ex-situ* through-plane conductivities, the greater water absorption of the sPPB-50 PEM appears to negatively impact its performance. This can be attributed not only to the substantial increase in WU when saturated with water during cell operation, but also to differences in membrane morphology. The organization of ionic domains within the membrane, along with the hydrophilic-hydrophobic phase separation within the material, significantly influences water and proton transport through the membrane, thus impacting its overall performance [32]. The presence of the reinforcement layer in Pemion-15 and Pemion-40 evidently affects these properties, promoting better water transport through the membranes. Further investigations on the morphology of these PEMs are warranted for a better understanding of the effects of incorporating a structural reinforcing layer. A detailed comparison of the water electrolyzer performance of the Pemion-based CCMs with other fluorine-free sulfonated polyarylene polymers in PEMWE is reported in Table S1.

The durability of Pemion-based and N112-based water electolyzer cells were compared by holding the current density at 1 A cm^{-2} and monitoring the voltage changes for 100 h [52]. Previous reports have examined the use of various sulfonated polyarylene polymers for PEMWE, with a few mentioning the electrolyzers durability (Table S1). A 74 μm PEEK-Reinforced sulfonated poly(phenylene sulfone) membrane recently reported the lowest degradation rate (0.08 mV h^{-1}) for a hydrocarbon-based polymer after 649 h of operation in a PEMWE [53]. The corresponding voltage change for all the MEAs under study is shown

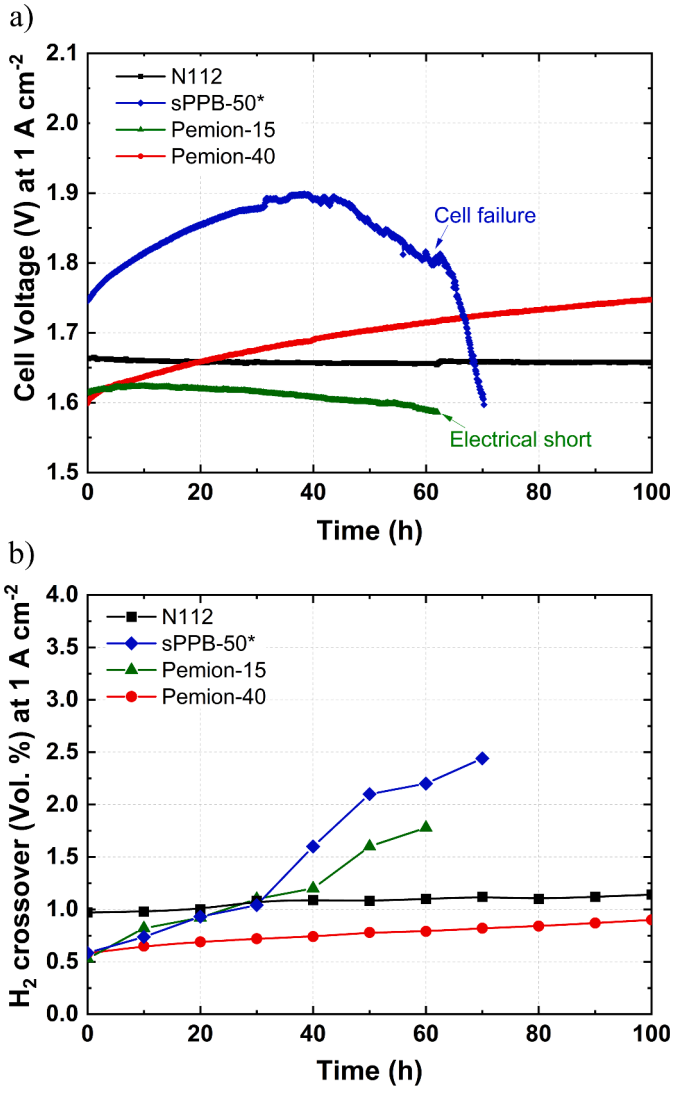

Fig. 3. a) Durability at 1 A cm^{-2} and 70 °C with ambient pressure, water flow rate of 200 mL min^{-1} for Pemion-15, Pemion-40, sPPB-50, and N112 membrane CCMs. b) Gas crossover measurements of anodic gas using gas chromatography. The gas was collected during the durability studies at 10 h intervals. MEAs contained ~3.0 mg Ir cm^{-2} + 10 wt% Nafion™ D520 dispersion in the anode, and ~1.0 mg Pt cm^{-2} + 20 wt% Nafion D520™ dispersion in the cathode catalyst layer.
*Data from reference [33].

in Fig. 3(a). The Pemion-15 CCM initially displayed a minimal degradation rate of 0.002 mV h^{-1} during the first 10 h, however, it consistently developed electrical short-circuiting after 20–40 h of operation. After analyzing four CCMs, 60 h was the longest stable data could be obtained without short-circuiting the cell. This issue can be traced back to the thin thickness of the Pemion-15 membrane, making it susceptible to pinholes due to its inherently lower quantity of material, leading to worsened structural integrity and diminished durability. The Pemion-40 CCM exhibited a voltage evolution rate of 1.46 mV h^{-1} during 100 h of operation, while the N112 CCM possessed a voltage evolution rate of

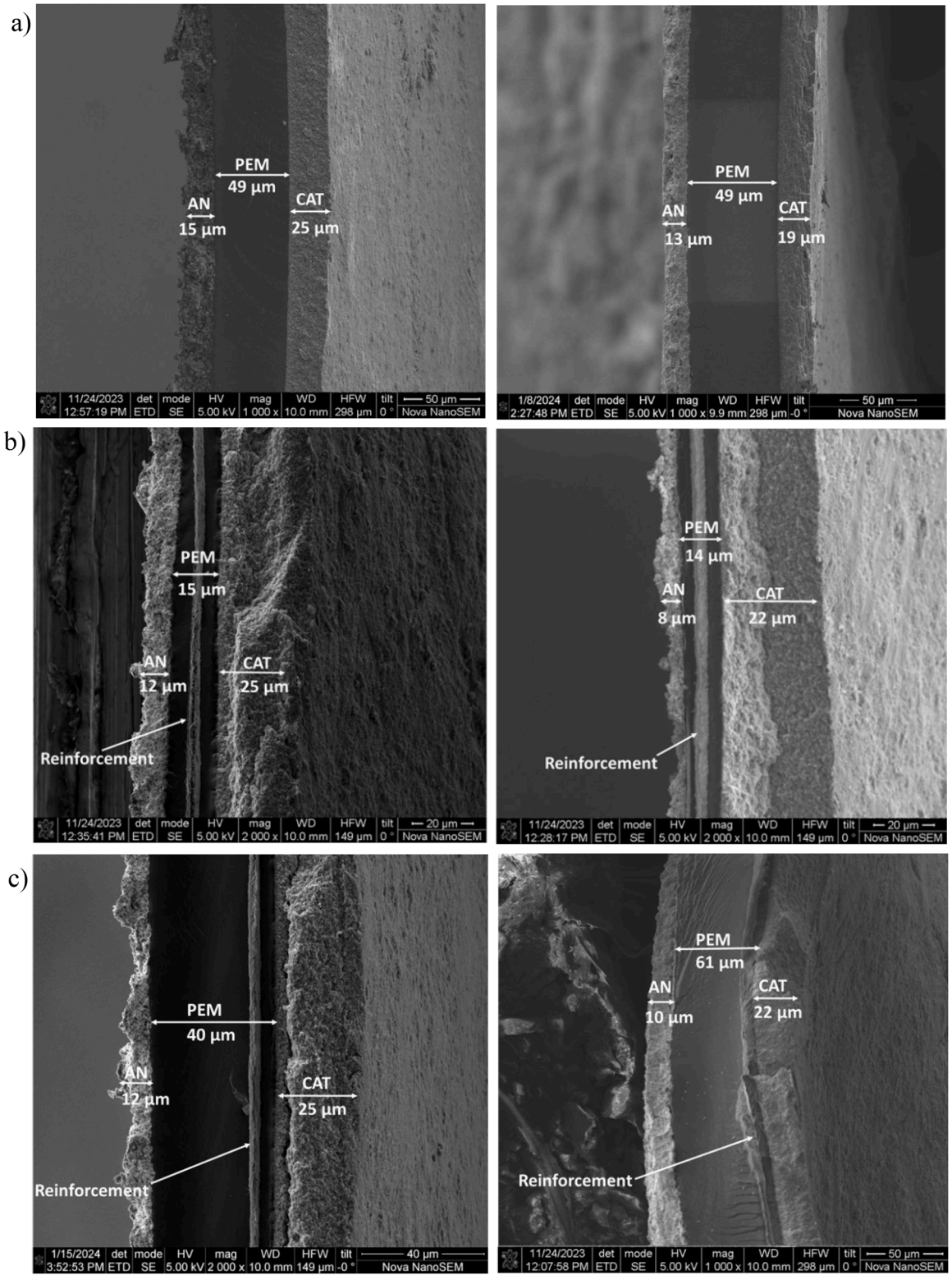

Fig. 4. a) Cross-sectional SEM of fresh (left) and used (right) N112 CCM. The used CCM shows the catalyst layer and minimal loss of the catalyst layer after 100 h operation. b) Cross-sectional SEM of fresh (left) and used (right) Pemion-15 CCM. The CCM exhibited signs of catalyst layer delamination in the form of cracks after a 60 h operation. c) Cross-sectional SEM of fresh (left) and used (right) Pemion-40 CCM. The CCM exhibited signs of catalyst layer delamination after a 100 h operation.

0.06 mV h^{-1}. The Pemion-40 membrane CCM showed a significantly improved durability compared to the previously reported sPPB-50 membrane which had a much higher voltage increase by 3.29 mV h^{-1} at 1 A cm^{-2} over the first 40 h and degraded rapidly after 60 h [33]. The improved stability of the Pemion-40 membrane compared to sPPB-50 can be attributed to its enhanced mechanical integrity, characterized by diminished in-plane swelling, as a result of the added reinforcement layer, leading to a reduction of catalyst layer delamination [27]. However, the higher voltage degradation rate compared to N112 highlights the need for a more stable hydrocarbon-based ionomer for water electrolysis applications.

During water electrolysis operation, it is important to monitor the hydrogen crossover rate through the membrane, as it directly impacts cell performance [54,55]. To assess the crossover rate, the gaseous exhaust of the anode during chronopotentiometry at 1 A cm^{-2} was collected to analyze the volume of H_2 in O_2 (vol%) over time, as depicted in Fig. 3(b). In the previous work, while the sPPB-50 membrane initially demonstrated low gas crossover, it increased substantially to approximately 2.5 vol% after 30 h, which was attributed to its high dimensional swelling by the authors [33]. Similarly, in our study, Pemion-15 CCM showed a gas crossover of < 1 vol% within the first 10 h, which progressively increased to ~2 vol% over time during the 60 h durability test, possibly due to pinholes formation [56], leading to the above mentioned short circuit. On the other hand, Pemion-40 CCM exhibited a significantly lower hydrogen crossover (< 1 vol% of H_2 in O_2) during the 100-hour durability test. This markedly reduced hydrogen crossover contrasts with Pemion-15, sPPB-50, and N112 CCMs, which all displayed hydrogen crossover exceeding 1 vol%.

SEM cross-sectional images of the CCMs before and after durability studies are presented in Fig. 4**.** Post-durability images revealed reductions in the thickness of both the cathode and anode catalyst layers primarily attributable to delamination events within the CCMs. N112 CCM (Fig. 4a) showed negligible catalyst layer delamination compared to Pemion CCMs, with preservation of the CCM after 100 h of cell operation. Pemion-15 (Fig. 4b) and Pemion-40 (Fig. 4c) CCMs possessed evidence of cracks and loss of catalyst layer after the durability studies. The SEM images also demonstrate that the initial dry thickness of Pemion-40 was 40 μm, increased to 61 μm after the 100-hour operation, whereas N112 maintained the same thickness. Although Pemion-40 exhibited lower H_2 crossover than N112, its high water uptake is presumed to have led to increased mechanical stress on the CCM, resulting in catalyst layer disintegration, which contributes to degradation of the CCM [57]. In addition, upon cell disassembly, it was observed that a substantial fraction of the anode catalyst had migrated to the porous transport layer (Ti-felt), indicative of delamination from the Pemion CCMs; in contrast to the minimal delamination observed for the N112 membrane CCM (Fig. S3). The delamination of the catalyst layer of hydrocarbon-based membranes utilizing Nafion-based ionomers in the catalyst layers has been reported to be a result of poor compatibility between the hydrocarbon membranes and the Nafion-based ionomers [58,59]. These findings suggest a promising prospect that enhanced durability of PFSA-free CCMs could be achieved if there was a more effective synergy between the membrane and ionomeric material in the catalyst layer. Further research on ionomeric materials in the catalyst layer is therefore warranted.

4. Conclusions

This study significantly contributes to advancing the development of sustainable proton-exchange membranes (PEMs) for water electrolysis through the introduction of “Pemion-reinforced” fluorine-free membranes. The study tackles both the key drawbacks of traditional fluorinated PEMs, such as Nafion™ 112, which are potentially harmful to the environment, and the poor mechanical and electrochemical stability of current fluorine-free polymer membranes such as sPPB-50. Our study showcases that Pemion-40 exhibits improved performance and reduced hydrogen gas crossover, enhancing the efficiency of the water electrolyzer device when compared to Nafion™ 112 (N112) membrane. It has also shown superior proton conductivity than commercial standard N112 and minimized water electrolyzer voltage loss during operation when compared to the non-reinforced sPPB-50 membrane. The enhanced durability is due to the structural reinforcement which does not compromise proton transport properties. Electrolysis cells containing Pemion-15 and Pemion-40 membranes exhibited a voltage of 1.60 V at 1 A cm^{-2} in comparison to 1.68 V obtained with the N112-based MEA and 1.66 V for non-reinforced sPPB-50-based MEA at the same current density. Over 100 h of operation at 1 A cm^{-2}, Pemion-40 catalyst coated membrane (CCM) exhibited hydrogen crossover below 1 vol. % with a voltage evolution rate of 1.46 mV hr^{-1}. Pemion-15 CCM initially displayed a promisingly minimal degradation rate of 0.002 mV h^{-1} during the first 10 h, however, it consistently developed electrical short-circuiting after a few hours of operation due to its very thin thickness. Challenges related to water uptake and catalyst layer delamination were identified, indicating the need for further optimization to enhance the long-term durability of these materials. The results underscore the critical role of reinforcement supports in improving the performance of fluorine-free PEMs, offering a sustainable pathway for hydrogen production. Moreover, exploring the compatibility between membrane and ionomeric materials for catalyst layers holds promise for improving overall performance and extending the lifespan of PEMWE technologies.

CRediT authorship contribution statement

Franklin O. Egemole: Writing – review & editing, Writing – original draft, Methodology, Investigation, Formal analysis, Data curation. **Ana Laura G. Biancolli:** Writing – review & editing, Writing – original draft, Visualization, Validation. **Steven Holdcroft:** Writing – review & editing, Supervision, Resources, Project administration, Methodology, Funding acquisition, Conceptualization.

Declaration of competing interest

The authors declare the following financial interests/personal relationships which may be considered as potential competing interests:

Steven Holdcroft reports financial support was provided by Natural Sciences and Engineering Research Council of Canada. Ana Laura G. Biancolli reports financial support was provided by State of Sao Paulo Research Foundation. Steven Holdcroft reports a relationship with Ionomr Innovations Inc that includes: consulting or advisory. SH is a co-founder of, and scientific advisor to, Ionomr Innovations Inc, the supplier of the reinforced sulfo-phenylated polyphenylene membranes used in this work. If there are other authors, they declare that they have no known competing financial interests or personal relationships that could have appeared to influence the work reported in this paper.

Acknowledgements

This research was funded by the Natural Sciences and Engineering Research Council of Canada (NSERC) through Discovery Grant RGPIN-2018-03698. A.L.G.B. acknowledges FAPESP grants No. 2019/26955-3 and 2021/14786-2 and CINE/SHELL (ANP)/FAPESP grant No. 2017/11937- 4.

Supplementary materials

Supplementary material associated with this article can be found, in the online version, at doi:10.1016/j.electacta.2024.145259.

References

[1] Q. Feng, X.Z. Yuan, G. Liu, B. Wei, Z. Zhang, H. Li, et al., A review of proton exchange membrane water electrolysis on degradation mechanisms and mitigation

strategies, J. Power Sources 366 (2017), https://doi.org/10.1016/j.jpowsour.2017.09.006.
[2] K. Ayers, The potential of proton exchange membrane–based electrolysis technology, Curr. Opin. Electrochem. 18 (2019), https://doi.org/10.1016/j.coelec.2019.08.008.
[3] M. Carmo, D.L. Fritz, J. Mergel, D. Stolten, A comprehensive review on PEM water electrolysis, Int. J. Hydrogen Energy 38 (2013), https://doi.org/10.1016/j.ijhydene.2013.01.151.
[4] Bessarabov D., Wang H., Li H., Zhao N. PEM electrolysis for hydrogen production: principles and applications. 2016. https://doi.org/10.1201/b19096.
[5] A. Makhsoos, M. Kandidayeni, B.G. Pollet, L. Boulon, A perspective on increasing the efficiency of proton exchange membrane water electrolyzers– a review, Int. J. Hydrogen Energy 48 (2023), https://doi.org/10.1016/j.ijhydene.2023.01.048.
[6] S. Garbe, J. Futter, T.J. Schmidt, L. Gubler, Insight into elevated temperature and thin membrane application for high efficiency in polymer electrolyte water electrolysis, Electrochim. Acta 377 (2021), https://doi.org/10.1016/j.electacta.2021.138046.
[7] U. Babic, M. Suermann, F.N. Büchi, L. Gubler, T.J. Schmidt, Critical review—identifying critical gaps for polymer electrolyte water electrolysis development, J. Electrochem. Soc. 164 (2017), https://doi.org/10.1149/2.1441704jes.
[8] M. Suermann, T.J. Schmidt, F.N. Büchi, Cell performance determining parameters in high pressure water electrolysis, Electrochim. Acta 211 (2016), https://doi.org/10.1016/j.electacta.2016.06.120.
[9] A. Kusoglu, A.Z. Weber, New insights into perfluorinated sulfonic-acid ionomers, Chem. Rev. 117 (2017), https://doi.org/10.1021/acs.chemrev.6b00159.
[10] M.F. Ahmad Kamaroddin, N. Sabli, T.A. Tuan Abdullah, S.I. Siajam, L.C. Abdullah, A. Abdul Jalil, et al., Membrane-based electrolysis for hydrogen production: a review, Membranes (Basel) 11 (2021), https://doi.org/10.3390/membranes11110810.
[11] S. Siracusano, N. Van Dijk, R. Backhouse, L. Merlo, V. Baglio, A.S. Aricò, Degradation issues of PEM electrolysis MEAs, Renew. Energy 123 (2018), https://doi.org/10.1016/j.renene.2018.02.024.
[12] F.D. Coms, The chemistry of fuel cell membrane chemical degradation, ECS Trans. 16 (2008), https://doi.org/10.1149/1.2981859.
[13] D. Dhanapal, M. Xiao, S. Wang, Y. Meng, A review on sulfonated polymer composite/organic-inorganic hybrid membranes to address methanol barrier issue for methanol fuel cells, Nanomaterials 9 (2019), https://doi.org/10.3390/nano9050668.
[14] H. Ito, T. Maeda, A. Nakano, H. Takenaka, Properties of Nafion membranes under PEM water electrolysis conditions, Int. J. Hydrogen Energy 36 (2011), https://doi.org/10.1016/j.ijhydene.2011.05.127.
[15] R. Nolte, K. Ledjeff, M. Bauer, R. Mülhaupt, Partially sulfonated poly(arylene ether sulfone) - a versatile proton conducting membrane material for modern energy conversion technologies, J. Memb. Sci. 83 (1993), https://doi.org/10.1016/0376-7388(93)85268-2.
[16] C.A. Linkous, H.R. Anderson, R.W. Kopitzke, G.L. Nelson, Development of new proton exchange membrane electrolytes for water electrolysis at higher temperatures, Int. J. Hydrogen Energy 23 (1998), https://doi.org/10.1016/s0360-3199(97)00113-4.
[17] R. Kumar, M. Mamlouk, K. Scott, Sulfonated polyether ether ketone-sulfonated graphene oxide composite membranes for polymer electrolyte fuel cells, RSC Adv. 4 (2014), https://doi.org/10.1039/c3ra42390e.
[18] J.E. Park, J. Kim, J. Han, K. Kim, P.S. Bin, S. Kim, et al., High-performance proton-exchange membrane water electrolysis using a sulfonated poly(arylene ether sulfone) membrane and ionomer, J. Memb. Sci. 620 (2021), https://doi.org/10.1016/j.memsci.2020.118871.
[19] S.Y. Han, D.M. Yu, Y.H. Mo, S.M. Ahn, J.Y. Lee, T.H. Kim, et al., Ion exchange capacity controlled biphenol-based sulfonated poly(arylene ether sulfone) for polymer electrolyte membrane water electrolyzers: comparison of random and multi-block copolymers, J. Memb. Sci. 634 (2021), https://doi.org/10.1016/j.memsci.2021.119370.
[20] C. Klose, T. Saatkamp, A. Münchinger, L. Bohn, G. Titvinidze, M. Breitwieser, et al., All-hydrocarbon MEA for PEM water electrolysis combining low hydrogen crossover and high efficiency, Adv. Energy Mater. 10 (2020), https://doi.org/10.1002/aenm.201903995.
[21] G. Wei, L. Xu, C. Huang, Y. Wang, SPE water electrolysis with SPEEK/PES blend membrane, Int. J. Hydrogen Energy 35 (2010), https://doi.org/10.1016/j.ijhydene.2010.05.041.
[22] K. Ayers, N. Danilovic, R. Ouimet, M. Carmo, B. Pivovar, M. Bornstein, Perspectives on low-temperature electrolysis and potential for renewable hydrogen at scale, Annu. Rev. Chem. Biomol. Eng. 10 (2019), https://doi.org/10.1146/annurev-chembioeng-060718-030241.
[23] Y. Chen, C. Liu, J. Xu, C. Xia, P. Wang, B.Y. Xia, et al., Key components and design strategy for a proton exchange membrane water electrolyzer, Small Struct. 4 (2023) 2200130, https://doi.org/10.1002/sstr.202200130.
[24] E.J. Park, C.G. Arges, H. Xu, Y.S. Kim, Membrane strategies for water electrolysis, ACS Energy Lett. 7 (2022), https://doi.org/10.1021/acsenergylett.2c01609.
[25] X. Li, Z. Zhang, Z. Xie, X. Guo, T. Yang, Z. Li, et al., High performance and self-humidifying of novel cross-linked and nanocomposite proton exchange membranes based on sulfonated polysulfone, Nanomaterials 12 (2022), https://doi.org/10.3390/nano12050841.
[26] H. Zhu, M. Jia, Q. Li, C. Zhang, P. Zheng, Research the effect of crosslinking degree on the overall performance of novel proton exchange membranes, Solid State Ion. 351 (2020), https://doi.org/10.1016/j.ssi.2020.115325.
[27] S.J. Hong, H.Y. Jung, S.J. Yoon, K.H. Oh, S.G. Oh, Y.T. Hong, et al., Constrained hydrocarbon-based ionomers in porous poly(tetrafluoroethylene) supports for enhanced durability of polymer electrolyte membrane fuel cells and water electrolyzers, J. Power Sources 551 (2022), https://doi.org/10.1016/j.jpowsour.2022.232221.
[28] S.H. Kang, H.Y. Jeong, S.J. Yoon, S. So, J. Choi, T.H. Kim, et al., Hydrocarbon-based composite membrane using LCP-nonwoven fabrics for durable proton exchange membrane water electrolysis, Polymers (Basel) 15 (2023), https://doi.org/10.3390/polym15092109.
[29] E. Balogun, P. Mardle, H. Nguyen, M. Breitwieser, S. Holdcroft, Catalyst layers for fluorine-free hydrocarbon PEMFCs, Electrochim. Acta 401 (2022), https://doi.org/10.1016/j.electacta.2021.139479.
[30] E. Balogun, M. Adamski, S. Holdcroft, Communication—non-fluorous, hydrocarbon PEMFCs, generating >1 W cm −2 Power, J. Electrochem. Soc. 167 (2020), https://doi.org/10.1149/1945-7111/ab88bd.
[31] E. Balogun, S. Holdcroft, Impact of conditioning protocol on hydrocarbon-based solid polymer electrolyte fuel cells, J. Power Sources 570 (2023), https://doi.org/10.1016/j.jpowsour.2023.233008.
[32] M. Adamski, N. Peressin, S. Holdcroft, On the evolution of sulfonated polyphenylenes as proton exchange membranes for fuel cells, Mater. Adv. 2 (2021), https://doi.org/10.1039/d1ma00511a.
[33] X. Wang, P. Mardle, M. Adamski, B. Chen, S. Holdcroft, Proton exchange membrane water electrolysis incorporating sulfo-phenylated polyphenylene catalyst coated membranes, J. Electrochem. Soc. 170 (2023) 024502, https://doi.org/10.1149/1945-7111/acb643.
[34] S.H. Mirfarsi, A. Kumar, J. Jeong, M. Adamski, S. McDermid, B. Britton, et al., High-temperature stability of hydrocarbon-based Pemion® proton exchange membranes: a thermo-mechanical stability study, Int. J. Hydrogen Energy 50 (2024), https://doi.org/10.1016/j.ijhydene.2023.07.236.
[35] P.M. Falcone, M. Hiete, A. Sapio, Hydrogen economy and sustainable development goals: review and policy insights, Curr. Opin. Green Sustain. Chem. 31 (2021), https://doi.org/10.1016/j.cogsc.2021.100506.
[36] M. Adamski, T.J.G. Skalski, B. Britton, T.J. Peckham, L. Metzler, S. Holdcroft, Highly stable, low gas crossover, proton-conducting phenylated polyphenylenes, Angew. Chem. - Int. Ed. 56 (2017), https://doi.org/10.1002/anie.201703916.
[37] E. Rasten, G. Hagen, R. Tunold, Electrocatalysis in water electrolysis with solid polymer electrolyte, Electrochim. Acta 48 (2003), https://doi.org/10.1016/j.electacta.2003.04.001.
[38] P. Wen, Z. Zhong, L. Li, F. Shen, X.D. Li, M.H. Lee, A novel approach to prepare photocrosslinked sulfonated poly(arylene ether sulfone) for proton exchange membrane, J. Memb. Sci. 463 (2014), https://doi.org/10.1016/j.memsci.2014.03.042.
[39] Y.S. Kim, Polymer electrolytes with high ionic concentration for fuel cells and electrolyzers, ACS Appl. Polym. Mater. 3 (2021), https://doi.org/10.1021/acsapm.0c01405.
[40] H.C. Lee, H.S. Hong, Y.M. Kim, S.H. Choi, M.Z. Hong, H.S. Lee, et al., Preparation and evaluation of sulfonated-fluorinated poly(arylene ether)s membranes for a proton exchange membrane fuel cell (PEMFC), Electrochim. Acta 49 (2004), https://doi.org/10.1016/j.electacta.2004.01.012.
[41] A. Sadeghi Alavijeh, S. Bhattacharya, O. Thomas, C. Chuy, E. Kjeang, A rapid mechanical durability test for reinforced fuel cell membranes, J. Power Sources Adv. 2 (2020), https://doi.org/10.1016/j.powera.2020.100010.
[42] M. Wang, W. Ma, C. Yang, Z. Xia, S. Wang, G. Sun, Study on fiber-reinforced proton exchange membrane using high-surface-energy substrate, J. Memb. Sci. 647 (2022), https://doi.org/10.1016/j.memsci.2021.119940.
[43] A.L.G. Biancolli, A. Konovalova, E.I. Santiago, S. Holdcroft, Measuring the ionic conductivity of solid polymer electrolyte powders, Int. J. Electrochem. Sci. 18 (2023), https://doi.org/10.1016/J.IJOES.2023.100288.
[44] S.H. Yun, S.H. Shin, J.Y. Lee, S.J. Seo, S.H. Oh, Y.W. Choi, et al., Effect of pressure on through-plane proton conductivity of polymer electrolyte membranes, J. Memb. Sci. (2012) 417–418, https://doi.org/10.1016/j.memsci.2012.06.041.
[45] T. Soboleva, Z. Xie, Z. Shi, E. Tsang, T. Navessin, S. Holdcroft, Investigation of the through-plane impedance technique for evaluation of anisotropy of proton conducting polymer membranes, J. Electroanal. Chem. 622 (2008), https://doi.org/10.1016/j.jelechem.2008.05.017.
[46] K. Cooper, Characterizing through-plane and in-plane ionic conductivity of polymer electrolyte membranes, ECS Meet. Abstr. (2011), https://doi.org/10.1149/ma2011-02/16/1043. MA2011-02.
[47] R. Sigwadi, T. Mokrani, M.S. Dhlamini, P. Nonjola, P.F. Msomi, Nafion®/sulfated zirconia oxide-nanocomposite membrane: the effects of ammonia sulfate on fuel permeability, J. Polym. Res. 26 (2019), https://doi.org/10.1007/s10965-019-1760-2.
[48] C. Wang, S. Young Lee, D. Won Shin, N. Rae Kang, Y.M. Lee, M.D. Guiver, Proton-conducting membranes from poly(ether sulfone)s grafted with sulfoalkylamine, J. Memb. Sci. 427 (2013), https://doi.org/10.1016/j.memsci.2012.09.040.
[49] Y.S. Noh, H.Y. Jeong, S.J. Yoon, H.J. Kim, Y.T. Hong, J. Choi, et al., Multilayered hydrocarbon ionomer/PTFE composite electrolytes with enhanced performance for energy conversion devices, Int. J. Hydrogen Energy 48 (2023), https://doi.org/10.1016/j.ijhydene.2022.11.038.
[50] L. Ma, S. Sui, Y. Zhai, Investigations on high performance proton exchange membrane water electrolyzer, Int. J. Hydrogen Energy 34 (2009), https://doi.org/10.1016/j.ijhydene.2008.11.022.
[51] S. Siracusano, S. Trocino, N. Briguglio, V. Baglio, A.S. Aricò, Electrochemical impedance spectroscopy as a diagnostic tool in polymer electrolyte membrane electrolysis, Materials (Basel) 11 (2018), https://doi.org/10.3390/ma11081368.

[52] Q. Feng, X.Z. Yuan, G. Liu, B. Wei, Z. Zhang, H. Li, et al., A review of proton exchange membrane water electrolysis on degradation mechanisms and mitigation strategies, J. Power Sources 366 (2017), https://doi.org/10.1016/j.jpowsour.2017.09.006.

[53] R. Qelibari, E.C. Ortiz, N. van Treel, F. Lombeck, C. Schare, A. Münchinger, et al., 74 μm PEEK-reinforced sulfonated poly(phenylene sulfone)-membrane for stable water electrolysis with lower gas crossover and lower resistance than Nafion N115, Adv. Energy Mater. 14 (2024) 2303271, https://doi.org/10.1002/aenm.202303271.

[54] S.A. Grigoriev, V.I. Porembskiy, S.V. Korobtsev, V.N. Fateev, F. Auprêtre, P. Millet, High-pressure PEM water electrolysis and corresponding safety issues, Int. J. Hydrogen Energy 36 (2011), https://doi.org/10.1016/j.ijhydene.2010.03.058.

[55] K.D. Baik, B.K. Hong, M.S. Kim, Effects of operating parameters on hydrogen crossover rate through Nafion® membranes in polymer electrolyte membrane fuel cells, Renew. Energy 57 (2013), https://doi.org/10.1016/j.renene.2013.01.046.

[56] S.A. Grigoriev, K.A. Dzhus, D.G. Bessarabov, P. Millet, Failure of PEM water electrolysis cells: case study involving anode dissolution and membrane thinning, Int. J. Hydrogen Energy 39 (2014), https://doi.org/10.1016/j.ijhydene.2014.05.043.

[57] G.H. Byun, J.A. Kim, N.Y. Kim, Y.S. Cho, C.R. Park, Molecular engineering of hydrocarbon membrane to substitute perfluorinated sulfonic acid membrane for proton exchange membrane fuel cell operation, Mater. Today Energy 17 (2020), https://doi.org/10.1016/j.mtener.2020.100483.

[58] K.A. Sung, W.K. Kim, K.H. Oh, J.K. Park, The catalyst layer containing sulfonated poly(ether ether ketone) as the electrode ionomer for polymer electrolyte fuel cells, Electrochim. Acta 54 (2009), https://doi.org/10.1016/j.electacta.2009.01.024.

[59] E.B. Easton, T.D. Astill, S. Holdcroft, Properties of gas diffusion electrodes containing sulfonated poly(ether ether ketone), J. Electrochem. Soc. 152 (2005), https://doi.org/10.1149/1.1864412.